Bioorganic & Medicinal Chemistry Letters 22 (2012) 5714–5720

Contents lists available at SciVerse ScienceDirect

Bioorganic & Medicinal Chemistry Letters

journal homepage: www.elsevier.com/locate/bmcl

Synthesis and structure–activity relationships of dual PI3K/mTOR inhibitors based on a 4-amino-6-methyl-1,3,5-triazine sulfonamide scaffold

Ryan P. Wurz [a,*], Longbin Liu [a], Kevin Yang [a], Nobuko Nishimura [a], Yunxin Bo [a], Liping H. Pettus [a], Sean Caenepeel [b], Daniel J. Freeman [b], John D. McCarter [b], Erin L. Mullady [b,e], Tisha San Miguel [b], Ling Wang [b], Nancy Zhang [b], Kristin L. Andrews [c], Douglas A. Whittington [c,e], Jian Jiang [d], Raju Subramanian [d], Paul E. Hughes [b], Mark H. Norman [a]

[a] Department of Chemistry Research & Discovery, Amgen Inc., One Amgen Center Drive, Thousand Oaks, CA 91320, USA
[b] Department of Oncology, Amgen Inc., One Amgen Center Drive, Thousand Oaks, CA 91320, USA
[c] Department of Molecular Structure, Amgen Inc., One Amgen Center Drive, Thousand Oaks, CA 91320, USA
[d] Department of Pharmacokinetics & Drug Metabolism, Amgen Inc., One Amgen Center Drive, Thousand Oaks, CA 91320, USA
[e] Amgen Inc., 360 Binney St., Cambridge, MA 02142, USA

ARTICLE INFO

Article history:
Received 7 May 2012
Revised 21 June 2012
Accepted 25 June 2012
Available online 3 July 2012

Keywords:
Phosphoinositide 3-kinase
Mammalian target of rapamycin
PI3K
mTOR
Sulfonamide
Triazine
Oncology

ABSTRACT

Phosphoinositide 3-kinase (PI3K) is an important target in oncology due to the deregulation of the PI3K/Akt signaling pathway in a wide variety of tumors. A series of 4-amino-6-methyl-1,3,5-triazine sulfonamides were synthesized and evaluated as inhibitors of PI3K. The synthesis, in vitro biological activities, pharmacokinetic and in vivo pharmacodynamic profiling of these compounds are described. The most promising compound from this investigation (compound **3j**) was found to be a pan class I PI3K inhibitor with a moderate (>10-fold) selectivity over the mammalian target of rapamycin (mTOR) in the enzyme assay. In a U87 MG cellular assay measuring phosphorylation of Akt, compound **3j** displayed low double digit nanomolar IC_{50} and exhibited good oral bioavailability in rats (F_{oral} = 63%). Compound **3j** also showed a dose dependent reduction in the phosphorylation of Akt in a U87 tumor pharmacodynamic model with a plasma EC_{50} = 193 nM (91 ng/mL).

The family of lipid kinases termed phosphatidylinositol 3-kinases (PI3Ks) catalyze the phosphorylation of the 3-hydroxyl position of phosphatidylinositides and play key regulatory roles in many cellular processes including cell survival, nutrient uptake, proliferation and differentiation.[1] The PI3K family consists of at least eight proteins that share sequence homology within their kinase domains and yet have distinct substrate specificities and modes of regulation.[5] The best characterized members of this family are the four class I PI3Ks (α, β, γ and δ isoforms) that link PI3K activity to a large variety of cell-surface receptors, comprised of growth factor receptors as well as G protein-coupled receptors (GPCRs).[2] There is significant evidence that the PI3K/Akt pathway is deregulated in many human cancers.[3–5] For example, the gene encoding the p110α subunit, PIK3CA, is amplified and overexpressed in several cervical, gastric, and ovarian cancer cell lines and is mutated in a wide variety of other cancers including breast, colorectal, glioblastoma, and gastric cancers.[4] In addition, PI3K signaling is negatively regulated by the lipid phosphatase PTEN, which is one of the most commonly mutated proteins in human malignancy, providing further evidence for the role of the PI3K pathway in cancer. Hence, inhibition of PI3K, and in particular its p110α subunit, is a promising target for cancer therapeutics.[6,7] Many industrial and academic groups have pursued both selective PI3K[8] and dual PI3K/mTOR inhibitors,[9] and several of these inhibitors have advanced to Phase II clinical trials.[10]

In a previous communication, we reported the results of our structure–activity relationship (SAR) efforts that focused on the optimization of a series of sulfonamides appended to a benzothiazole scaffold derived from an initial high-throughput screening lead from Amgen's proprietary sample bank.[11] These efforts resulted in the discovery of compound **1** which was a potent dual inhibitor of class I PI3Ks and mTOR (Fig. 1). However, subsequent pharmacokinetic studies revealed that compound **1** underwent deacetylation in vivo resulting in the formation of an active metabolite, which complicated further development efforts.[12a] In addition, the low solubility of compound **1** (0.001, 0.001 and

* Corresponding author. Tel.: +1 805 313 5400; fax: +1 805 480 1337.
E-mail address: rwurz@amgen.com (R.P. Wurz).

0960-894X/$ - see front matter © 2012 Elsevier Ltd. All rights reserved.
http://dx.doi.org/10.1016/j.bmcl.2012.06.078

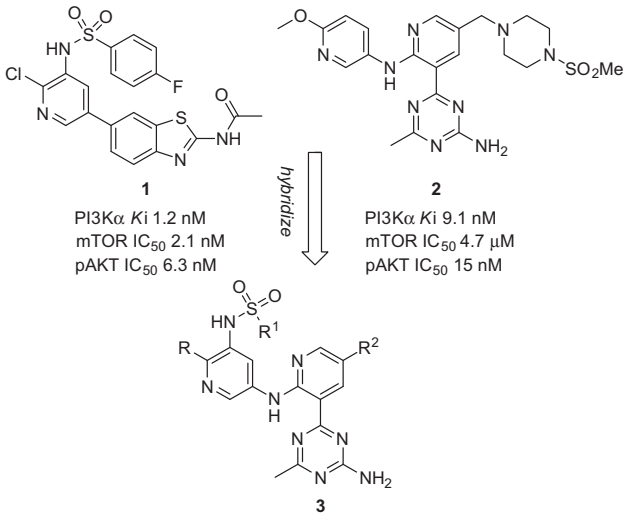

Figure 1. Hybridization of compounds **1** and **2** leading to the discovery of the 4-amino-6-methyl-1,3,5-triazine sulfonamide class of inhibitors (**3**).

0.013 mg/mL, in 0.01 N HCl, phosphate buffer (PBS) and simulated intestinal fluid (SIF), respectively, Table 3) may have contributed to the compound's low oral bioavailability (F_{oral} = 12%).[13] Although formulation efforts on compound **1** eventually led to improved oral exposures through the use of a pH adjustment,[14] the long-term stability of the resulting suspension also presented a development challenge. We postulated that the presence of the acetamide hydrogen bond donor-acceptor functionality coupled with the fused bicyclic aromatic ring system of the *N*-acetyl benzothiazole may contribute to the decreased solubility of this series. Therefore, we proposed replacing the *N*-acetyl benzothiazole functionality of compound **1** with a different linker system that lacked these features, thereby eliminating the inherent deacetylation liability as well as providing a potential means to enhance the solubility of the molecules. Improved solubility could help increase the rate of dissolution of a molecule and lead to better oral bioavailability. Based on these considerations, we set out to explore a different linker system for the sulfonamide series.[12]

Separately, we have identified a second generation of PI3K inhibitors resulting from optimization of a lead exemplified by compound **2**.[15] Compound **2** was a potent pan class I PI3K inhibitor and was selective against mTOR. While compound **2** had improved solubility (0.2, 0.006, 0.007 mg/mL in 0.01 N HCl, PBS and SIF, respectively) over compound **1**, it had moderate in vivo pharmacokinetic (PK) properties (CL = 1.7 L/h/kg in rats). We believed that one possible approach to addressing the shortcomings of both of these inhibitors was to pursue a hybrid strategy exemplified by generic structure **3** wherein the chloropyridyl sulfonamide affinity pocket moiety of **1** replaced the 2-methoxypyridyl group of **2** (Fig. 1).

Insight into the possible mode of binding for this proposed hybrid came from the X-ray co-crystal structures of compounds **1** and **2** in PI3Kγ, displayed in Figure 2.[16] In the case of compound **1**, the *N*-acetyl benzothiazole group, also referred to as the 'linker binder' moiety, forms two key hydrogen bonds with the backbone NH and carbonyl of Val882. In this pair of interactions, the thiazole nitrogen acts as the hydrogen bond acceptor and the NH of the *N*-acetyl group serves as the hydrogen bond donor.[11] Whereas in compound **2**, the 4-amino-6-methyl-1,3,5-triazine motif interacts with the Val882 residue.[12,17] Both compounds contain a pyridine moiety whose nitrogen engages in a hydrogen bond with a water molecule bridging between Tyr867 and Asp841 in the 'affinity pocket'.

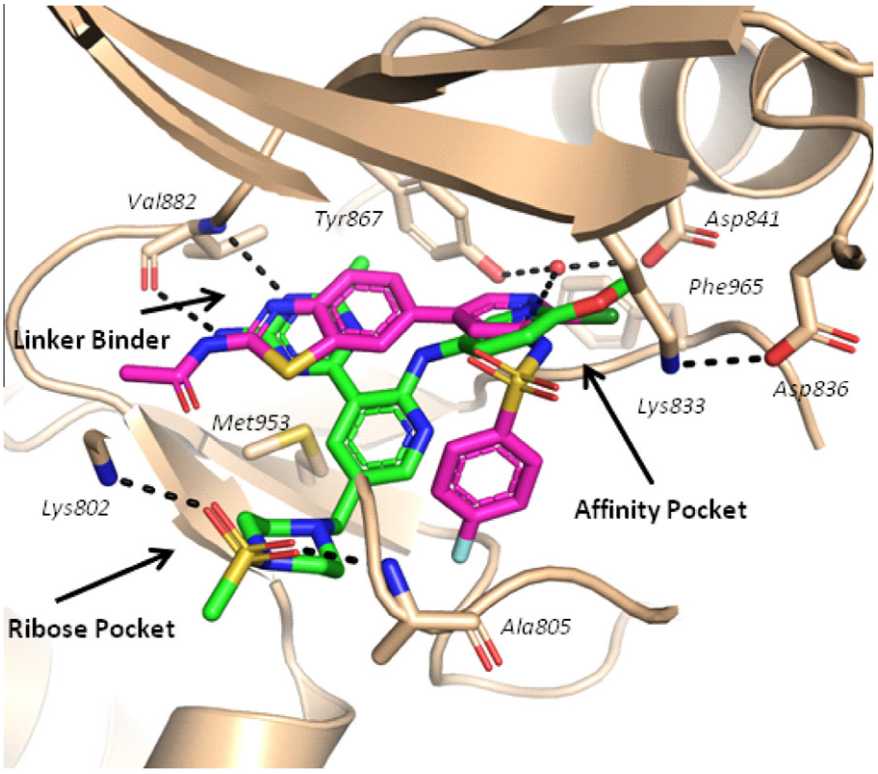

Figure 2. Overlay of the X-ray co-crystal structures of compounds **1** and **2** in the ATP binding site of unphosphorylated PI3Kγ determined to 2.85 Å and 2.95 Å resolution, respectively. PDB codes: 3QK0 and 4DK5. Dashed lines indicate hydrogen bonds. For inhibitor **1**, C: pink; N: blue; O: red; S: yellow; F: light blue; Cl: dark green. For inhibitor **2**, C: green; N: blue; O: red; S: yellow.

Table 1
Enzyme and cellular assay results for compounds arising from modifications to the sulfonamide of the affinity pocket binding motif

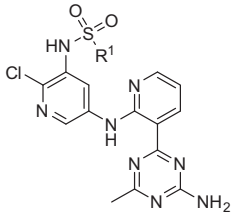

Compd	R^1	PI3Kα K_i (nM) [a]	pAkt (U87 MG) IC_{50} (nM)[a]	*c*Log*P*	Cell shift
3a	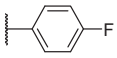	16	187	2.9	11.7
3b		20	20	1.0	1.0
3c		11	36	1.6	3.3
3d		11	25	1.4	2.3
3e		43	408	2.2	9.5
3f		16	85	1.8	5.3

[a] Data represents an average of at least two separate determinations.

Table 2
Enzyme and cellular assay results arising from modifications to the ribose pocket binding motif

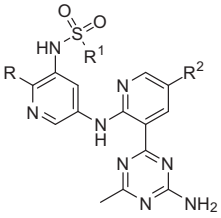

Compd	R	R^1	R^2	PI3K K_i (nM)[a]	pAkt (U87 MG) IC_{50} (nM)[a]	*c*Log*P*
3g				3.5	18	1.7
3h				161	95	1.5
3i				114	95	2.3
3j				12	24	2.1
3k				13	380	2.5
3l				29	53	2.3
3m				8.6	248	2.5
3n				11[b]	3.9	1.4
3o				9.3	6.3	1.8
3p				13	7.6[b]	2.2
3q				25	7.7[b]	1.3
3r				2.0	1.4[b]	1.2
3s				9.7	5.3[b]	0.8
3t				1.9	3.9[b]	1.1

[a] Data represents an average of at least two separate determinations.
[b] Data represents a single measurement.

Compound **2** exploits the 'ribose pocket' of the ATP binding pocket with a methyl(methanesulfonylpiperazine) group appended to the 5-position of the pyridine central ring.

Herein, we report the synthesis and biological evaluation of a series of compounds based on hybrid structure **3**. Initially we focused on inhibitors designed to explore the affinity pocket in which the ribose pocket was unelaborated (R^2 = H, Table 1). In subsequent analogs, substituents were introduced to take advantage of the ribose pocket in an attempt to improve potency, solubility and PK properties (Table 2).

Analogs were prepared in a straightforward manner according to Scheme 1. The 5-amino-pyridinyl-3-sulfonamide building blocks **6** were accessed from commercially available 3-amino-5-bromopyridines **4** followed by treatment with the desired sulfonyl chlorides. Transformation of bromides **5** into amines **6** involved the palladium-catalyzed cross-coupling of bromides **5** with benzophenone imine[18] followed by hydrolysis with 1 N HCl. The triazine linker binder moiety was prepared using a Suzuki coupling[19] of 4-chloro-6-methyl-1,3,5-triazin-2-amine (**7**) with suitably functionalized 2-fluoropyridine boronic acids **8** furnishing 4-(2-fluoropyridin-3-yl)-6-methyl-1,3,5-triazin-2-amines **9**. Base-promoted S_NAr displacement of the 2-fluoropyridine **9** with the fully elaborated 5-amino-pyridinyl-3-sulfonamides **6** afforded inhibitors **3a–t**. In this manner, three points of diversity (R, R^1 and R^2) necessary for analoging could be accessed in a relatively modular fashion.[20]

The inhibitory activities of the PI3Kα enzyme for all compounds were determined using a modified in vitro AlphaScreen assay.[11] The cellular activities were determined with a U87 MG cell-based assay measuring the phosphorylation of Akt (pAkt) at serine-473 as a readout. The first compound (**3a**) in which we replaced the 2-methoxypyridine with the chloropyridinyl sulfonamide moiety in the affinity pocket displayed encouraging enzyme potency (PI3Kα *Ki* = 16 nM, Table 1); however, there was a 12-fold shift in potency in the U87 MG cell-based assay (pAkt IC_{50} = 187 nM). Although there are a number of factors, such as permeability, pK_a, and melting point, that could contribute to the large cell-shift, we postulated that the compound's relatively high *c*Log*P* = 2.9 maybe a contributing factor.[21] With this in mind, replacement of the 4-fluorophenylsulfonamide with a methylsulfonamide (compound **3b**) resulted in a compound whose *c*Log*P* value was substantially reduced (*c*Log*P* = 1.0). This compound exhibited nearly a 10-fold improvement in cell-shift when compared to compound **3a**. It is noteworthy to mention, the solubility of this compound was also markedly improved to 5.8, 2.9 and 46.2 mg/mL in 0.01 N HCl, PBS and SIF, respectively.

Other analogs were prepared with small groups for R^1. A cyclopropyl sulfonamide (compound **3c**) was well tolerated, albeit a slightly greater cell-shift was observed as compared to compound **3b**. In a similar fashion, the *N,N*-dimethylamino-sulfonamide analog (compound **3d**) was equipotent to **3b** in both enzyme and cellular assays; however, further elaboration to an *iso*-propylmethylamino- or a morpholinylsulfonamide led to significant erosion in PI3Kα cellular potencies (compounds **3e–f**).

Preliminary results from Table 1 suggested small sulfonamide groups (R^1) were preferred in order to achieve cellular potencies <50 nM. To further probe the relationship between cellular

Table 3
Pharmacokinetic properties of selected compounds

Compd	In vitro liver Microsomal stability[a]		In vivo rat PK[b]				
	Rat	Human	iv[c]			po[d]	
	CL (μL/min/mg)	CL (μL/min/mg)	CL (L/h/kg)	Vdss (L/kg)	MRT (h)	%F	AUC (ng h/mL)
1	<20	<14	0.007	0.17	26.9	103	3200
2	9	6	1.7	2.6	1.6	77	1199
3b	<14	<14	0.39	0.40	4.5	33	4238
3j	27	47	0.39	0.97	2.5	63	3360
3n	<14	<14	0.21	0.28	1.3	1.8	419
3o	20	26	0.52	1.01	2.0	22	859
3q	<14	<14	0.46	0.52	1.1	28[e]	1210
3r	<14	<14	1.76	2.57	1.4	27	321

[a] Single experimental value; estimated clearance from percent parent compound (1 μM) remaining following a 30 min incubation in liver microsomes (0.25 mg/mL) and NADPH (1 mM).
[b] Pharmacokinetic parameters following administration in male Sprague Dawley rat; mean values from 3 animals per dosing route.
[c] Dosed at 1 mg/kg as a solution in DMSO.
[d] po doses were 2 mg/kg in 1% pluronic F68, 2% hydroxypropyl methylcellulose (HPMC), 15% hydroxypropyl β-cyclodextrin (HPBCD), 82% water/methanesulfonic acid pH 2.2.
[e] po dose was 2 mg/kg in 100% DMSO.

potency and physicochemical properties, introduction of polar groups to the 5-position of the central pyridine ring (R^2 of **3**) was explored as the crystallographic overlays of compounds **1** and **2** suggested that modifications to this portion of the inhibitor should be well tolerated (see Fig. 2). The first compound (**3g**) prepared in this series contained a chloride in the 5-position of the pyridine (R^2 = Cl). This compound was found to be equipotent to the parent compound (R^2 = H, compound **3b**) (Table 2). Compounds **3h–i** examined the influence of modifying the 2-substituent (R = Cl) on the affinity pocket binding motif. When the R-group was changed to Me or OMe, a >30-fold loss in enzyme potency resulted and additional modifications at this position were not pursued

Four additional analogs (compounds **3j–m**) containing the 5-chloropyridine substitution pattern (R^2 = Cl) as the central pyridine ring were examined and the potencies of the resulting compounds mirrored previous results from Table 1. The methoxyethylmethylamine sulfonamide (compound **3l**) was designed to improve solubility and was found to have modest enzyme potency on PI3Kα with a low cell-shift. The morpholinylsulfonamide (compound **3m**) exhibited improved solubility (1.0, 1.0 and 11.1 mg/mL in 0.01 N HCl, PBS and SIF, respectively) as compared to its unsubstituted analog (compound **3f**); however, a large cell-shift persisted.

The next modification was to introduce a methoxy-group to the 5-position of the pyridine central ring (R^2 = OMe) to reduce the *c*Log *P*. This modification reduced *c*Log *P* and decreased the cell-shift resulting in three compounds with single digit nanomolar potencies in the cell-based assay (compounds **3n–p**). The morpholinyl-sulfonamide (compound **3p**) displayed a much smaller cell-shift as compared to previous analogs (compound **3p** vs **3f** and **3m**). Further elaboration of the 5-methoxypyridine (R^2 = OMe) to a 5-methoxy-ethoxy-pyridine (**3q**, $R^2 = O(CH_2)_2OMe$) did not affect the cellular or enzyme potencies (compound **3q** vs **3n**).

To determine if additional gains in potency could be made through the judicious choice of the ribose pocket substitution (modifications to R^2), SAR generated from optimization of compound **2** was revisited and the analysis suggested hydrogen bond acceptors such as a tetrahydropyran or methylmorpholine could serve to improve potency.[16] Indeed, introduction of a tetrahydropyran into the ribose pocket resulted in compound **3r** that had excellent enzyme potency (PI3Kα *K*i = 2.0 nM) and cellular potency (pAkt IC_{50} = 1.4 nM).[22] A similar improvement in potency was also realized through the introduction of a methylmorpholine (compounds **3s–t**).

The X-ray structure of compound **3r** co-crystallized in PI3Kγ was obtained (Fig. 3). The expected interactions between the protein and the triazine linker binder are present as previously observed for compound **2**[16] forming two hydrogen bonds with the PI3Kγ residue Val882 of the linker region. The tetrahydropyran moiety projects into the ribose pocket and the 2-chloro-pyridyl-sulfonamide occupies the affinity pocket. Somewhat surprisingly, the catalytic Lys833 sits up and away from the inhibitor and makes only a weak hydrogen bond to an oxygen atom of the sulfone.[11,12,16,23] The sulfonamide motif sits in a pocket formed by the side chain of Lys833 and by Pro810, Met804, and Ser806. All of these residues are conserved across the class I PI3K's and all but one are conserved in mTOR (Met804 is Ile697 in mTOR). Although the water is unresolved, there are likely two hydrogen bonds formed via an ordered water molecule located between the chloropyridine ring nitrogen and the Tyr867 and Asp841 residues as previously observed for compound **1** (Fig. 2).[11] Comparison of the X-ray co-crystal stuctures of compound **2** and **3r** helps rationalize the preference for a 2-chloropyridine versus a 2-methyl- or 2-methoxy-pyridine (compound **3g** vs **3h** and **3i**).[24] The preference for the chloro-substitution in the hybrid series likely arises as a result of the affinity pocket binding motif lying deeper into the pocket than in compound **2**, thus the more sterically demanding

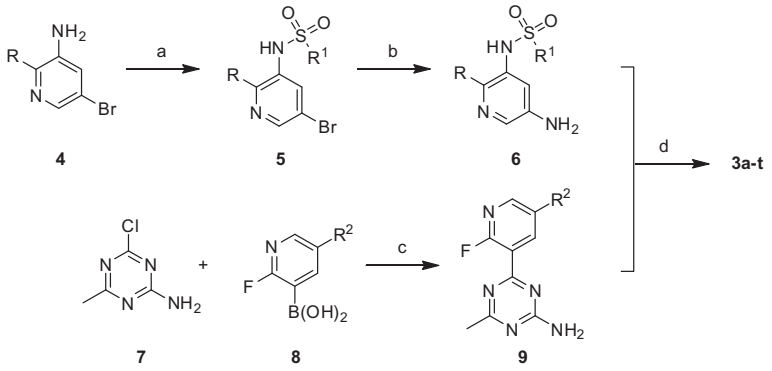

Scheme 1. General scheme for the synthesis of *N*-(5-((3-(4-amino-6-methyl-1,3,5-triazin-2-yl)pyridin-2-yl)amino)pyridin-3-yl)sulfonamides (**3**). Reagents and conditions: (a) R^1SO_2Cl, pyridine, DMAP; (b) (i) $Pd_2(dba)_3$ (5 mol %), Xantphos (10 mol %), benzophenone imine (1.1 equiv), NaO*t*-Bu (4 equiv), DMF, microwave, 140 °C, 20 min; (ii) THF, 1 N HCl, RT, 30 min; (c) (4-$NMe_2C_6H_4Pt$-$Bu_2)_2PdCl_2$ (Amphos, 5 mol %), KOAc (3 equiv), 100 °C, 1,4-dioxane, 16 h; (d) LiHMDS or NaHMDS (4 equiv.), DMF or THF, 0 °C to rt, 11–87%.

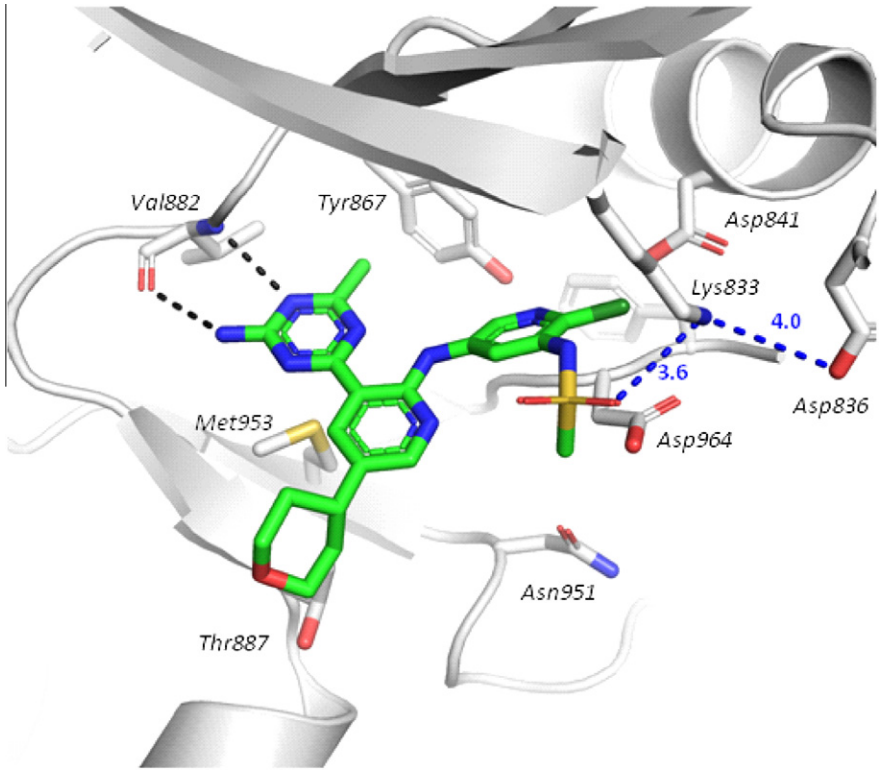

Figure 3. X-ray co-crystal structure of compound **3r** bound in the ATP binding site of unphosphorylated PI3Kγ determined to 3.0 Å resolution. PDB code: 4F1S. Dashed lines indicate hydrogen bonds (distances are in Angstroms). For the inhibitor, C: green; N: blue; O: red; S: yellow; Cl: dark green.

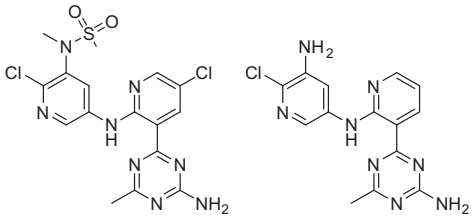

Figure 4. Additional modifications to the affinity pocket binding moiety.

2-methoxypyridine results in a decline in potency. Additionally, the 2-chloropyridine renders the sulfonamide nitrogen NH more acidic (pK_a = 5.7) than the corresponding 2-methylpyridine analog (pK_a = 6.9) thus favoring interaction with Lys833.

Two additional compounds were synthesized to further probe the importance of the sulfonamide group on the potency of the inhibitor. Compound **10**, wherein the nitrogen of the methylsulfonamide was methylated, was found to lose potency in the PI3Kα enzyme assay (PI3Kα K_i = 311 nM) (Fig. 4). This decline in potency could be the result of unfavorable interactions arising from projection of a hydrophobic methyl group toward the polar Lys833 residue. Additionally, the steric interaction between the 2-chloropyridine and the *N*-methylsulfonamide would alter the orientation of the sulfonamide group. Compound **11**, in which the sulfonamide was removed entirely, also resulted in substantial loss in potency as the affinity pocket is no longer optimally occupied.

The pharmacokinetic (PK) properties of some of the most potent compounds were examined (Table 3). Compound **3b** had low clearance (0.39 L/kg/h; 12% of liver blood flow), low volume of distribution (0.40 L/kg), and modest oral bioavailability (F_{oral} = 33%). This profile represented an improvement in oral exposure compared to compound **2**. Compound **3j** showed good solubility (1.0, 2.0 and 11.6 mg/mL, in 0.01 N HCl, PBS and SIF, respectively) and exhibited the most favorable PK profile of the compounds tested with an oral bioavailability of 63% and an improved volume of distribution (0.97 L/kg) as compared to compound **3b**. These favorable properties translated into an MRT of 2.5 h and significant oral exposure (AUC = 3340 ng h/mL). Three compounds (**3n**, **3o**, **3q**) that had limited solubility,[25] but good cellular potencies, all showed low to moderate bioavailabilities resulting in low oral exposures. Compound **3r** which had the best cellular potency, unfortunately, showed high clearance of 1.8 L/kg/h despite having excellent liver microsomal stability, suggesting a non-P450 clearance mechanism in rats.

The SAR investigations described above enabled the identification of several potent PI3K inhibitors with IC_{50} values ⩽ 50 nM in the U87 MG pAkt cellular assay and with favorable PK profiles. In addition to these compounds being potent inhibitors of PI3Kα, they were also potent inhibitors of the other class I PI3K isoforms

Table 4
In vitro (enzyme assay) profiles of selected compounds[a]

Compd	PI3K K_i (nM)				mTOR IC_{50} (nM)	hVps34 IC_{50} (nM)
	α	β	γ	δ		
3b	20	4.4	2.4	1.2	198	1288
3j	7.7	0.6	1.0	0.4	163	606
3o	9.3	4.7	2.2	1.1	74	—
3q	18	16	14	6.1	32	—

[a] Data represents an average of at least two separate determinations. Details of the assays were previously reported.[11]

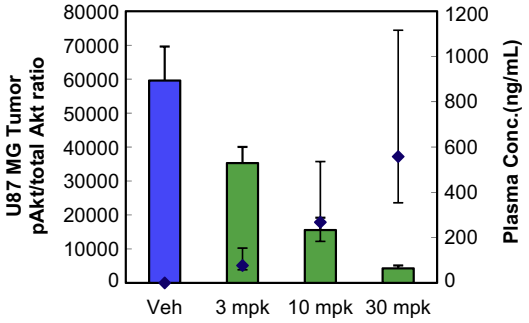

Figure 5. Effect of compound **3j** in a U87 tumor pharmacodynamic model measuring the inhibition of Akt (Ser 473) phosphorylation. Oral dose–response study at 6 h post-dose. Statistical significance was evaluated by Dunnett's method. Bars represent the average ± SD ($n = 3$).

(PI3Kβ, PI3Kγ and PI3Kδ) and mTOR (Table 4). As a general trend, the hybrid class of inhibitors of type **3** containing the *N*-(5-amino-2-chloropyridin-3-yl)sulfonamides were only modestly selective for PI3K over mTOR and had modest selectivity over hVps34, the class III PI3K.[26]

Based on the favorable rat PK properties of compound **3j**, it was chosen for testing in an in vivo mouse tumor pharmacodynamic (PD) model. Female CD1 nu/nu mice were implanted with U87 MG tumor cells (5×10^6 cells) and dosed orally with **3j** at 3, 10, and 30 mg/kg. Six hours post-dosing, tumor cells and plasma were harvested. Total Akt and pAkt (Ser473) levels in tumor were measured with a quantitative electrochemiluminescence immunoassay.[11] Compound **3j** showed a dose-dependent inhibition of Akt (Ser473) phosphorylation, indicating that it effectively inhibited PI3K in vivo (Fig. 5). The total plasma concentration for 50% tumor PD reduction (EC_{50}) in this experiment was calculated to be 193 nM (91 ng/mL; 95% CI: 116, 71 ng/mL).

The selectivity of compound **3j** against a panel of 50 protein and lipid kinases was examined in the AMBIT KINOME scan platform.[27] In this panel, the competitive binding of **3j** at 1 μM was measured as a percentage of control (POC). For all of the kinases assayed, no competitive binding (POC <50%) by **3j** was observed. Compound **3j** also showed moderate permeability and low efflux (12.2×10^{-6} cm/s and ER = 1.4 and 2.0, respectively in human and rodent LLC-PK1 cell line transfected with a MDR1 gene), and no hERG liability, but exhibited high plasma protein binding (99.8%, 99.8%, 99.65%, 97.13% in human, rat, dog and mouse, respectively).

In conclusion, a structurally novel class of pan class I PI3K inhibitors containing a 4-amino-6-methyl-1,3,5-triazine sulfonamide scaffold has been generated based on a molecular structure guided hybridization of the two previously reported classes of PI3K inhibitors. From this series, compound **3j** was highly selective against 50 other kinases and also had superior solubility properties over compound **1** and an improved PK profile over compound **2**. Compound **3j** was efficacious in a tumor PD assay in mice with an EC_{50} value of 193 nM (91 ng/mL).

Acknowledgments

The authors thank Randy Hungate, Terry Rosen, Rick Kendall, and Glenn Begley for their support of this research program. Thanks also go to Paul Andrews for his assistance with the in vitro cellular assays. In addition, we are grateful to Jin Tang and Peter Yakowec for expression and purification of the PI3Kγ enzyme.

Supplementary data

Supplementary data associated with this article can be found, in the online version, at http://dx.doi.org/10.1016/j.bmcl.2012. 06.078.

References and Notes

1. Crabbe, T.; Welham, M. J.; Ward, S. G. *Trends Biochem. Sci.* **2007**, *32*, 450.
2. Wymann, M. P.; Zvelebil, M.; Laffargue, M. *Trends Pharmacol. Sci.* **2003**, *24*, 366.
3. Vivanco, I.; Sawyers, C. L. *Nat. Rev. Cancer* **2002**, *2*, 489.
4. Liu, P.; Cheng, H.; Roberts, T. M.; Zhao, J. J. *Nat. Rev. Drug. Disc.* **2009**, *8*, 627.
5. Yap, T. A.; Garrett, M. D.; Walton, M. I.; Raynaud, F.; de Bono, J. S.; Workman, P. *Curr. Opin. Pharm.* **2008**, *8*, 393.
6. Ihle, N. T.; Powis, G. *Mol. Cancer Ther.* **2009**, *8*, 1.
7. Marone, R.; Cmiljanovic, V.; Giese, B.; Wymann, M. P. *Biochim. Biophys. Acta* **2008**, *1784*, 159.
8. For selected recent examples of selective PI3K inhibitors see: (a) Heffron, T. P.; Wei, B.; Olivero, A.; Staben, S. T.; Tsui, V.; Do, S.; Dotson, J.; Folkes, A. J.; Goldsmith, P.; Goldsmith, R.; Gunzner, J.; Lesnick, J.; Lewis, C.; Mathieu, S.; Nonomiya, J.; Shuttleworth, S.; Sutherlin, D. P.; Wan, N. C.; Wang, S.; Wiesmann, C.; Zhu, D.-Y. *J. Med. Chem.* **2011**, *54*, 7815; (b) Folkes, A. J.; Ahmadi, K.; Alderton, W. K.; Alix, S.; Baker, S. J.; Box, G.; Chuckowree, I. S.; Clarke, P. A.; Depledge, P.; Eccles, S. A.; Friedman, L. S.; Hayes, A.; Hancox, T. C.; Kugendradas, A.; Lensun, L.; Moore, P.; Olivero, A. G.; Pang, J.; Patel, S.; Pergl-Wilson, G. H.; Raynaud, F. I.; Robson, A.; Saghir, N.; Salphati, L.; Sohal, S.; Ultsch, M. H.; Valenti, M.; Wallweber, H. J. A.; Wan, N. C.; Wiesmann, C.; Workman, P.; Zhyvoloup, A.; Zvelebil, M. J.; Shuttleworth, S. J. *J. Med. Chem.* **2008**, *51*, 5522; (c) Knight, Z. A.; Chiang, G. G.; Alaimo, P. J.; Kenski, D. M.; Ho, C. B.; Coan, K.; Abraham, R. T.; Shokat, K. M. *Bioorg. Med. Chem.* **2004**, *12*, 4749.
9. For selected recent examples of dual PI3K/mTOR inhibitors see: (a) Sutherlin, D. P.; Bao, L.; Berry, M.; Castanedo, G.; Chuckowree, I.; Dotson, J.; Folks, A.; Friedman, L.; Goldsmith, R.; Gunzner, J.; Heffron, T.; Lesnick, J.; Lewis, C.; Mathieu, S.; Murray, J.; Nonomiya, J.; Pang, J.; Pegg, N.; Prior, W. W.; Rouge, L.; Salphati, L.; Sampath, D.; Tian, Q.; Tsui, V.; Wan, N. C.; Wang, S.; Wei, B.; Wiesmann, C.; Wu, P.; Zhu, B.-Y.; Olivero, A. *J. Med. Chem.* **2011**, *54*, 7579; (b) Sutherlin, D. P.; Sampath, D.; Berry, M.; Castanedo, G.; Chang, Z.; Chuckowree, I.; Dotson, J.; Folkes, A.; Friedman, L.; Goldsmith, R.; Heffron, T.; Lee, L.; Lesnick, J.; Lewis, C.; Mathieu, S.; Nonomiya, J.; Olivero, A.; Pang, J.; Prior, W. W.; Salphati, L.; Sideris, S.; Tian, Q.; Tsui, V.; Wan, N. C.; Wang, S.; Wiesmann, C.; Wong, S.; Zhu, B.-Y. *J. Med. Chem.* **2010**, *53*, 1086; (c) Maira, S.-M.; Stauffer, F.; Brueggen, J.; Furet, P.; Schnell, C.; Fritsch, C.; Brachmann, S.; Chène, P.; De Pover, A.; Schoemaker, K.; Fabbro, D.; Gabriel, D.; Simonen, M.; Murphy, L.; Finan, P.; Sellers, W.; García-Echeverría, C. *Mol. Cancer Ther.* **2008**, *7*, 1851.
10. (a) Holmes, D. *Nat. Rev. Drug Disc.* **2011**, *10*, 563; (b) Courtney, K. D.; Corcoran, R. B.; Engelman, J. A. *J. Clin. Oncol.* **2010**, *28*, 1075.
11. D'Angelo, N. D.; Kim, T.-S.; Andrews, K.; Booker, S. K.; Caenepeel, S.; Chen, K.; Freeman, D.; Jiang, J.; McCarter, J. D.; San Miguel, T.; Mullady, E. L.; Schrag, M.; Subramanian, R.; Tang, J.; Wahl, R. C.; Wang, L.; Whittington, D. A.; Wu, T.; Xi, N.; Xu, Y.; Yakowec, P.; Zalameda, L. P.; Zhang, N.; Hughes, P.; Norman, M. H. *J. Med. Chem.* **2011**, *54*, 1789.
12. Additional efforts towards this goal resulted in the exploration of an imidazolopyridazine scaffold, see: (a) Stec, M. M.; Andrews, K. L.; Booker, S. K.; Caenepeel, S.; Freeman, D. J.; Jiang, J.; Liao, H.; McCarter, J.; Mullady, E. L.; San Miguel, T.; Subramanian, R.; Tamayo, N.; Wang, L.; Yang, K.; Zalameda, L. P.; Zhang, N.; Hughes, P. E.; Norman, M. H. *J. Med. Chem.* **2011**, *54*, 5174; Quinoline/quinoxaline scaffolds were also evaluated, see: (b) Nishimura, N.; Siegmund, A.; Liu, L.; Yang, K.; Bryan, M. C.; Andrews, K. L.; Bo, Y.; Booker, S. K.; Caenepeel, S.; Freeman, D.; Liao, H.; McCarter, J.; Mullady, E. L.; San Miguel, T.; Subramanian, R.; Tamayo, N.; Wang, L.; Whittington, D. A.; Zalameda, L.; Zhang, N.; Hughes, P. E.; Norman, M. H. *J. Med. Chem.* **2011**, *54*, 4735.
13. The initial formulation was: 20% captisol, 2% HPMC, 1% Tween 80.
14. The formulation was the same as ref. 13 except dissolve compound **1** at pH 9.0 then readjust pH to 7.0.
15. Smith, A. L.; D'Angelo, N. D.; Bo, Y. Y.; Booker, S. K.; Cee, V. J.; Herberich, B.; Hong, F.-T.; Jackson, C. L. M.; Lanman, B. A.; Liu, L.; Nishimura, N.; Pettus, L. H.; Reed, A. B.; Tadesse, S.; Tamayo, N. A.; Wurz, R. P.; Yang, K.; Andrews, K. L.; Whittington, D. A.; McCarter, J. D.; San Miguel, T.; Zalameda, L.; Jiang, J.; Subramanian, R.; Mullady, E. L.; Caenepeel, S.; Freeman, D. J.; Wang, L.; Zhang, N.; Wu, T.; Hughes, P. E.; Norman, M. H. *J. Med. Chem.* **2012**, *55*, 5188.
16. PI3Kγ is used as the more amenable surrogate protein whose structure is highly homologous to PI3Kα. Residue numbers in the text refers to the PI3Kγ isoform. The X-ray crystal structure of PI3Kα has been reported, see: Huang, C.-H.; Mandelker, D.; Schmidt-Kittler, O.; Samuels, Y.; Velculescu, V. E.; Kinzler, K. W.; Vogelstein, B.; Gabelli, S. B.; Amzel, L. M. *Science* **2007**, *318*, 1744.
17. A structurally related linker binder moiety has been reported in PF-04691502, see: (a) Cheng, H.; Bagrodia, S.; Bailey, S.; Edwards, M.; Hoffman, J.; Hu, Q.; Kania, R.; Knighton, D. R.; Marx, M. A.; Ninkovic, S.; Sun, S.; Zhang, E. *Med. Chem. Commun.* **2010**, *1*, 139; See also: (b) Liu, K. K. C.; Huang, X.; Bagrodia, S.; Chen, J. H.; Greasley, S.; Cheng, H.; Sun, S.; Knighton, D.; Rodgers, C.; Rafidi, K.; Zou, A.; Xiao, J.; Yan, S. *Bioorg. Med. Chem. Lett.* **2011**, *21*, 1270.
18. Bhagwanth, S.; Adjabeng, G. M.; Hornberger, K. R. *Tetrahedron Lett.* **2009**, *50*, 1582.
19. (a) Guram, A. S.; King, A. O.; Allen, J. G.; Wang, X.; Schenkel, L. B.; Chan, J.; Bunel, E. E.; Faul, M. M.; Larsen, R. D.; Martinelli, M. J.; Reider, P. J. *Org. Lett.* **2006**, *8*, 1787; (b) Guram, A. S.; Wang, X.; Bunel, E. E.; Faul, M. M.; Larsen, R. D.; Martinelli, M. J. *J. Org. Chem.* **2007**, *72*, 5104.
20. For detailed experimental procedures see: Andrews, K.; Bo, Y. Y.; Booker, S.; Cee, V. J.; D'Angelo, N.; Herberich, B. J.; Hong, F.-T.; Jackson, C. L. M.; Lanman, B. A.; Liao, H.; Liu, L.; Nishimura, N.; Norman, M. H.; Pettus, L. H.; Reed, A. B.;

Smith, A. L.; Tadesse, S.; Tamayo, N. A.; Wu, B.; Wurz, R.; Yang, K. WO 2010126895, November 4, 2010.
21. Physicochemical properties were calculated using the Daylight Toolkit, within Amgen's proprietary software (ADAPT). For more information see: (a) Daylight Chemical Information Systems Inc. http://www.daylight.com.; (b) Cho, S. J.; Sun, Y.; Harte, W. J. *Comput.-Aided Mol. Des.* **2006**, *20*, 249.
22. It should be noted that the inhibition of phosphorylation of Akt (pAkt) at S473 of PTEN-null cell lines, such as U87 MG, are also sensitive to mTOR inhibition, therefore the cell IC50 values can be a composite of the various PI3K isoforms as well as mTOR, see: Neshat, M. S.; Mellinghoff, I. K.; Tran, C.; Stiles, B.; Thomas, G.; Petersen, R.; Frost, P.; Gibbons, J. J.; Wu, H.; Sawyers, C. L. *Proc. Natl. Acad. Sci. U.S.A.* **2001**, *98*, 10314.
23. Knight, S. D.; Adams, N. D.; Burgess, J. L.; Chaudhari, A. M.; Darcy, M. G.; Donatelli, C. A.; Luengo, J. I.; Newlander, K. A.; Parrish, C. A.; Ridgers, L. H.; Sarpong, M. A.; Schmidt, S. J.; Van Aller, G. S.; Carson, J. D.; Diamond, M. A.; Elkins, P. A.; Gardiner, C. M.; Garver, E.; Gilbert, S. A.; Gontarek, R. R.; Jackson, J. R.; Kershner, K. L.; Luo, L.; Raha, K.; Sherk, C. S.; Sung, C.-M.; Sutton, D.; Tummino, P. J.; Wegrzyn, R. J.; Auger, K. R.; Dhanak, D. *ACS Med. Chem. Lett.* **2010**, *1*, 39.
24. See Supplementary data for a superposition of the X-ray co-crystal structures of compounds **2** and **3r** in PI3Kγ.
25. For solubility data of selected potent PI3K inhibitors see the Supplementary data.
26. Backer, J. M. *Biochem. J.* **2008**, *410*, 1.
27. For more information, see: http://www.discoverx.com/technology/technology-kinomescan.php. The Ambit kinase panel included: Abl, Akt1, Akt2, AMPK, AurA, BTK, CAMK2, CAMK4, CDC7, CDK2, CHK1, CK1δ, CHK2, DYRK1α, Erk1, Erk2, FGFR1, FLT3, FYN, GSK3, HGK, IGF1R, INSR, IRAK4, KDR, LCK, LYN, MAPKAPK2, MARK1, MET, MSK1, MST2, p38α, p70S6 K, PAK2, PIM2, PKAC2, PKC, PKCβ2, PKD2, PKGα, PRAK, RAF, ROCK2, RSK1, SGK1, SRC, SYK, TAK1.